Adaptive Bayesian State Estimation Integrating Non-stationary DGNSS Inter-Agent Distances

Adaptive Bayesian State Estimation Integrating Non-stationary DGNSS Inter-Agent Distances

Simone Zocca
Dept. of Electronics and Telecommunications
Politecnico di Torino, Turin, Italy
simone.zocca@polito.it

Alex Minetto
Dept. of Electronics and Telecommunications
Politecnico di Torino, Turin, Italy
alex.minetto@polito.it

Fabio Dovis
Dept. of Electronics and Telecommunications
Politecnico di Torino, Turin, Italy
fabio.dovis@polito.it

***Abstract*—Bayesian navigation filters are broadly exploited in precise state estimation for kinematic applications such as vehicular positioning and navigation. Among these, Particle Filter (PF) has been shown as a valuable solution to support hybrid positioning algorithms such as sensor fusion to Global Navigation Satellite System (GNSS) and Cooperative Positioning (CP). Despite of an increased computational complexity w.r.t. conventional Kalman Filters (KFs), an effective weighting of the input measurements generally provides an improved accuracy of the output estimate. In the framework of the Differential GNSS (DGNSS) CP, this work presents an algorithm for the automated selection of the most appropriate error models for the tight-integration of non-stationary Differential GNSS (DGNSS) collaborative inter-agent distances. A model switching technique named Automated Adaptive Likelihood Switch (AALS) is proposed for a Cognitive Particle Filter (C-PF) architecture, based on the real-time approximation of the statistics of the inter-agent distances errors. The results achieved through realistic simulations demonstrated the effectiveness of the proposed solution in terms of error model selection. Therefore, an improvement of the position estimation accuracy was observed, since the cases in which DGNSS-CP would degrade performance due to possible mismodelling of the selected likelihood function are avoided.**

***Index Terms*—Bayesian estimation, Particle filter, adaptive estimation, global navigation satellite system, positioning and navigation**

I. Introduction

Positioning, navigation and timing are of the utmost importance to support the fast pace of a reliable, connected mobility [1]. In order to achieve improved accuracy in navigation, Global Navigation Satellite System (GNSS) must overcome its intrinsic limitations regarding the lack of visible satellites and degraded signals quality in harsh environment (i.e. mild-urban scenarios and urban canyons) [2].

Despite of the extensive effort devoted to the fusion of inertial sensors and GNSS, absolute positioning solutions still suffer from the aforementioned impairments. Therefore, the integration of auxiliary range information to the positioning problem have been investigated to compensate for such limitations [3], [4]. Indeed, along with relative bearing, inter-agent distances are the most diffused source of auxiliary information to improve localisation capabilities in standalone or cooperative multi-agent systems. Pioneering implementations first demonstrated the effectiveness of their integration in navigation units in the field of robotics [5] and later in vehicular technologies [6], whenever such data can be distributed through ad-hoc, low-latency links (e.g. Direct Short Range Communication (DSRC) based on IEEE 802.11p) [7], [8] or alternative, pre-existent network infrastructures. In the most popular applications, inter-agent distances are estimated through Radio-Frequency (RF) ranging via Ultra-Wide Band (UWB) transceivers [9], vision-based ranging or less reliably through the Round-trip Time (RTT) or Received Signal Strength (RSS) of Wi-Fi signals [10]. With the aim of overcoming Line-of-Sight (LoS) and coverage constraints of sensor-based ranging, recent research works proposed the exchange of GNSS observables among multiple agents.

Since in principle GNSS receivers work independently, these measurements need to be synchronised at receiver side through consolidated DGNSS techniques, thus imposing a maximum latency bound on the transmission of such measurements [6], [11], [12]. The analysis of such a bound and of the message transmission protocols are out of the scope of this paper.

Along with the possibility of retrieving GNSS corrections for high-precision positioning (e.g. Differential Global Positioning System (GPS), Real Time Kinematics (RTK), Wide Area RTK), DGNSS approaches allow for the computation of inter-agent distances among generic networked receivers in a cooperative fashion. DGNSS-Cooperative Positioning (CP) hence represents a promising paradigm towards the enhancement of standalone GNSS positioning, leveraging on the well-known properties of common error cancellation offered by DGNSS measurements [13]. However, when sequential Bayesian navigation filters (i.e. Particle Filter (PF)) are considered for the tight integration of GNSS pseudoranges and DGNSS ranges, a rigorous modelling of such input measurements is of paramount importance to guarantee high-accuracy solutions and to limit possible injection of biases. Indeed, compared to other Bayesian filters, the PF has the capability to natively handle non-Gaussian and non-linear measurement models typically observed in DGNSS inter-agent distances. According to its architecture, PF can provide a more accurate solution dealing with scenarios where Kalman Filter (KF)-based navigation filters are not effective due to the Taylor linearization of the measurements model and the Gaussian approximation of the noise statistics which affect

the input measurements [14], [15]. In fact, early studies on DGNSS-CP confirmed that a proper choice of the Probability Density Function (PDF)s modelling the inter-agent distances was needed to ensure higher performance w.r.t. state-of-the-art hybridised Extended Kalman Filter (EKF) solutions [16]. This was achieved through an off-line estimation of the statistics of the inter-agent distances in a controlled simulation environment, and their subsequent integration through a C-PF. In order to automate the error model selection, this work provides a run-time automated algorithm to determine the best-matching distribution among a set of pre-defined models, thus making C-PF architectures adaptive w.r.t. to the relative position and velocity of the surrounding collaborating agents.

The remainder of this paper is structured as follows: Section II describes the fundamentals on DGNSS-based inter-agent distances and how they are integrated in a PF for DGNSS-CP. In Section III, the proposed approach is presented by discussing the statistical properties of the distance between the collaborating agents. A summary of numerical and realistic results are discussed in Section IV and conclusions are eventually drawn in Section V.

II. Theoretical Background

Given the positions, $\boldsymbol{\theta}_{a,k}$, $\boldsymbol{\theta}_{b,k}$ of two kinematic agents A and B at given time instant t_k, ranging techniques aim at estimating their *inter-agent distance* (a.k.a. baseline length)

$$d_{ab,k} = ||\mathbf{d}_{ab,k}|| = ||\boldsymbol{\theta}_{a,k} - \boldsymbol{\theta}_{b,k}|| \tag{1}$$

where the operator $||\cdot||$ is the Euclidean norm and $\boldsymbol{\theta}_a$, $\boldsymbol{\theta}_b$ are the true locations of the two agents in a given Cartesian reference frame, as depicted in Figure 1. While RF-based

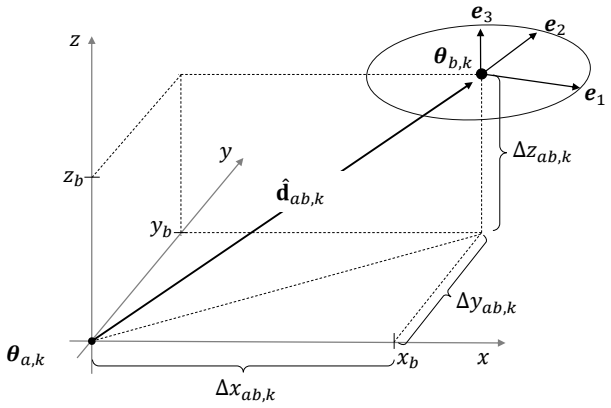

Fig. 1: Baseline vector and associated error covariance ellipsoid in a 3D Cartesian reference frame centered at the location of receiver A, $\boldsymbol{\theta}_a$.

solutions directly provide an estimate of (1) through the Time of Flight (ToF) or the RTT of the signal, conventional DGNSS techniques first estimate the quantity of interest

$$\mathbf{d}_{ab}(t_k) = \begin{bmatrix} \Delta x_{ab} & \Delta y_{ab} & \Delta z_{ab} \end{bmatrix} \tag{2}$$

and provide then an indirect estimate of (1), namely $\hat{d}_{ab,k}$, through the Euclidean norm of an estimate of (2).

A. DGNSS inter-agent distance estimation

Inter-agent distances computed through DGNSS techniques are far from being assumed stationary when kinematic conditions are experienced by the agents [16]. Their PDFs change according to the proximity of the cooperating GNSS receivers. This substantial difference requires a less trivial integration scheme of the measurements which must somehow take into account the relative position and speed of the cooperating agents [4]. Let assume two sets of S pseudorange measurements retrieved by two independent GNSS receivers, thus independently affected by additive noise terms modelled as uncorrelated Gaussian random vectors. It is worth recalling that such a "Gaussianity assumption" does not generally hold in real environments but it constitutes an ideal scenario (statistically-wise) in absence of multi-path phenomena. The measurements sets $\boldsymbol{\rho}_{a,k}$ and $\boldsymbol{\rho}_{b,k}$ are assumed to be retrieved at the same time instant, t_k, or to be aligned in post-processing by one of the agents, as proposed in [17]. The DGNSS estimation of inter-agent distances can be approached through few differential methods [18], based on the pseudorange measurements of independent GNSS receivers. Among the available techniques, the Weighted Double Difference Ranging (W-DDR) was chosen being suitable for the use with raw pseudorange measurements and the cancellation of all the systematic biases (i.e. receiver and satellites clock biases) [19]. In order to perform a W-DDR we first consider the single difference vector obtained subtracting the GNSS pseudorange measurements of the two receivers w.r.t. the set of shareable satellites [18].

$$\nabla_{ab,k} = \boldsymbol{\rho}_{a,k} - \boldsymbol{\rho}_{b,k}. \tag{3}$$

By assuming independent identically distributed input measurements, the error covariance matrix associated to ∇_{ab} is diagonal, with equal variance terms and it can be expressed as $\mathbf{R}_{\nabla} = 2\sigma_\rho^2 \mathbf{I}_{S\times S}$, where σ_ρ^2 is the variance associated to each pseudorange measurements. The computation of Double Differences (DD) measurements can be obtained through the linear combination $\nabla\Delta_{ab} = \mathbf{L}_{\nabla\Delta}\nabla_{ab}$, as

$$\underbrace{\begin{bmatrix} D^{12}_{ab,k} \\ D^{13}_{ab,k} \\ \vdots \\ D^{1(S-1)}_{ab,k} \end{bmatrix}}_{\nabla\Delta_{ab}} = \underbrace{\begin{bmatrix} -1 & 1 & 0 & \cdots & 0 \\ -1 & 0 & 1 & \ddots & 0 \\ \vdots & \vdots & \ddots & \ddots & \vdots \\ -1 & 0 & \cdots & \cdots & 1 \end{bmatrix}}_{\mathbf{L}_{\nabla\Delta}} \underbrace{\begin{bmatrix} S^1_{ab,k} \\ S^2_{ab,k} \\ S^3_{ab,k} \\ \vdots \\ S^S_{ab,k} \end{bmatrix}}_{\nabla_{ab}}. \tag{4}$$

and the error covariance matrix associated to $\nabla\Delta_{ab}$ is hence given by

$$\begin{aligned} \mathbf{R}_{\nabla\Delta} = \mathbf{L}_{\nabla\Delta}\mathbf{R}_{\nabla}\mathbf{L}^\top_{\nabla\Delta} &= 2\sigma_\rho^2 \left(\mathbf{L}_{\nabla\Delta}\mathbf{I}_{S\times S}\mathbf{L}^\top_{\nabla\Delta}\right) \\ &= 2\sigma_\rho^2 \left(\mathbf{1}_{V\times V} + \mathbf{I}_{V\times V}\right) \end{aligned} \tag{5}$$

where $\mathbf{L}_{\nabla\Delta}$ is the matrix describing the differencing operation among the set of single differences [12], $\mathbf{1}$ is a unitary matrix and $V = S - 1$, is the number of computable DDs using a predefined reference satellite. By neglecting the residual noise contribution affecting the DD, $\mathbf{d}_{ab,k}$ can be estimated

by collecting $S-1$ double difference measurements from a set of S satellites simultaneously visible to agents a and b, inverting

$$\nabla\Delta_{ab,k} \simeq \begin{bmatrix} \left[\mathbf{h}^2_{a,k} - \mathbf{h}^1_{b,k}\right] \\ \left[\mathbf{h}^3_{a,k} - \mathbf{h}^1_{b,k}\right] \\ \cdots \\ \left[\mathbf{h}^S_{a,k} - \mathbf{h}^1_{b,k}\right] \end{bmatrix} \mathbf{d}_{ab,k} \tag{6}$$

where the generic $\mathbf{h}^s_{r,k}$ is a unitary vector pointing to the s-th satellite from the location of the r-th receiver and part of the Direction Cosine Matrix (DCM) evaluated by the receivers for the conventional Position Time Velocity (PVT) computation [2]. Furthermore, by considering an effective selection of the *reference satellite* [16], the set of equations implied by the inversion of (6) can be solved through a Weighted Least Square (WLS) algorithm, as

$$\hat{\mathbf{d}}_{ab,k} = (\mathbf{H}^\top_{\nabla,k}\mathbf{W}\mathbf{H}_{\nabla,k})^{-1}\mathbf{H}^\top_{\nabla,k}\mathbf{W}\,\nabla\Delta_{ab,k} \tag{7}$$

where $\mathbf{H}_{\nabla,k}$ is the second term in (6), and $\mathbf{W} = \left[\mathbf{R}_d^{(\nabla\Delta)}\right]^{-1}$ is a weight matrix. An estimate of the inter-agent distance is then obtained by taking the Euclidean norm of (7). The computation of the error covariance matrix, $\mathbf{R}_d^{(\nabla\Delta)}$ of the baseline length is given by

$$\mathbf{R}_d^{(\nabla\Delta)} = \left(\mathbf{H}^\top_\nabla\mathbf{H}_\nabla\right)^{-1}\mathbf{H}^\top_\nabla\mathbf{R}_{\nabla\Delta}\mathbf{H}_\nabla\left(\mathbf{H}^\top_\nabla\mathbf{H}_\nabla\right)^{-1} \tag{8}$$

Generally, if i.i.d. pseudorange measurements are assumed as input, (8) is a fully-populated, positive definite matrix. It is worth remarking that the eigenvectors $\mathbf{e}_i$ of the error covariance matrix, $\mathbf{R}_d^{(\nabla\Delta)}$, are independent w.r.t. the direction of the baseline vector, as depicted in Figure 1. Their orientation depends on the geometry of the observed GNSS satellites and of the cooperating receivers, hence on the matrix $\mathbf{H}_\nabla$.

B. Variance Estimation of the Inter-agent Distance

Assuming unbiased input measurements, an estimate of the variance of the inter-agent distance would be sufficient to weight the contribution or to at least approximate a suitable PDF model. Unfortunately, there are no closed form to estimate the variance σ_d^2 of the Euclidean norm of a multivariate random vector from its covariance matrix. Therefore, a set of popular heuristics can be used to provide a quantitative analysis of σ_d^2:

- $\psi_1 = \frac{Tr\left(R_d^{(\nabla\Delta)}\right)}{k}$ The trace does not take into account the correlation of the differential terms in (2), therefore is suitable for diagonal error covariance matrices. See also [20], [21].
- $\psi_2 = |R_d^{(\nabla\Delta)}|^{1/3}$ where $|\cdot|$ is the determinant of the argument. It takes into account correlation terms [22]–[26].
- $\psi_3 = R_{d,11}^{(\nabla\Delta)}$. Accounts for the first term of the error covariance matrix.
- $\psi_4 = \lambda_1\left(R_d^{(\nabla\Delta)}\right)$ considers the first eigenvalue of the matrix which can be related to the variance along the most relevant axis of the multi-variate error distribution. It is typically used in principal component analysis.

These quantities can be used to only approximate the variance of an inter-agent distance, being alternative to a direct, signal-processing-oriented approach (e.g. windowed time-based estimation). The behaviour of the estimation error on the inter-agent distance is analyzed hereafter by varying both the value of the mean quantity and its estimated variance, ψ_2.

C. Bayesian Estimation through Cognitive Particle Filter

The sequential Bayesian estimation implemented through PFs is generally based on the processing of a set of particles aiming at modelling the statistics of the space state vector, according to the high-level scheme shown in Figure 2.

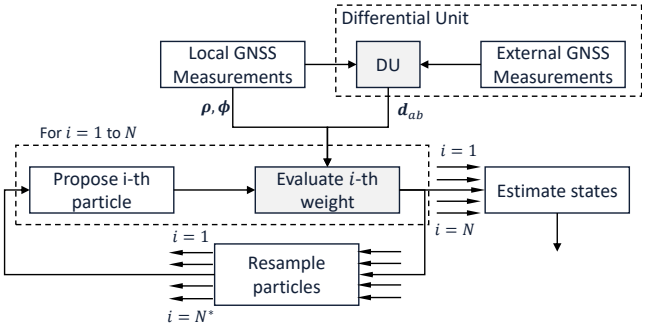

Fig. 2: Hybrid PF proposed in [27] and extended in [12] to implement the tight integration of non-stationary DGNSS inter-agent distances.

A hybrid state estimation based on PF can be performed by integrating DGNSS inter-agent distances, $\mathbf{d}_k$, with conventional GNSS pseudorange and Doppler measurements, $\mathbf{z}_k$, and optimising the PF for sensor-less navigation purposes [16]. The set of particles is generated over a spatial region according to a given statistical distribution:

$$\hat{\boldsymbol{\theta}}^i_k \sim \mathcal{D}(\mathbf{x}_{k-1}, \mathbf{P}_k) \tag{9}$$

where $\mathbf{x}_{k-1}$ is the previous state estimate, $\mathbf{P}_k$ is the *state covariance matrix* and $\mathcal{D}$ represents a generic statistical distributions (e.g. Gaussian, Rayleigh). The i-th particle $\hat{\boldsymbol{\theta}}^i_k$, represents a possible realisation of the state space vector at time t_k, defined as

$$\hat{\boldsymbol{\theta}}^i_k = [\mathrm{x}^i_k \quad \mathrm{y}^i_k \quad \mathrm{z}^i_k \quad \mathrm{b}^i_k \quad \dot{\mathrm{x}}^i_k \quad \dot{\mathrm{y}}^i_k \quad \dot{\mathrm{z}}^i_k \quad \dot{\mathrm{b}}^i_k] \tag{10}$$

where $\mathbf{x}^i_k = [\mathrm{x}^i_k \quad \mathrm{y}^i_k \quad \mathrm{z}^i_k]$ refers to the spatial coordinates, $\mathbf{v}^i_k = [\dot{\mathrm{x}}^i_k \quad \dot{\mathrm{y}}^i_k \quad \dot{\mathrm{z}}^i_k]$ to the axial velocity components, while b^i_k and $\dot{\mathrm{b}}^i_k$ are respectively the bias and drift of the local clock. After each particle $\hat{\boldsymbol{\theta}}^i_k$ is predicted following the dynamic system model, the nominal measurement vector $\hat{\mathbf{z}}^i_k$ is computed. Then, auxiliary ranges are integrated by appending them to $\mathbf{z}^i_k$, creating a new nominal measurements vector $\bar{\mathbf{z}}^i_k$ as

$$\bar{\mathbf{z}}^i_k = [\mathbf{z}^i_k \quad \mathbf{d}^i_k] = [\bar{z}_{1,k} \quad \bar{z}_{2,k} \ldots \bar{z}_{M,k}] \tag{11}$$

where M is the number of measurements in $\bar{\mathbf{z}}^i_k$. The weights are then obtained by relying on a pre-defined PDF,

$p\left(\bar{z}_{n,k}|\hat{\boldsymbol{\theta}}_k^i\right)$, w.r.t. the expected measurements computed for each particle. The normalised weights are hence defined as

$$w_k^i = \frac{\mathcal{L}(\bar{\mathbf{z}}_k|\hat{\boldsymbol{\theta}}_k^i)}{\sum_{i=1}^N \mathcal{L}(\bar{\mathbf{z}}_k|\hat{\boldsymbol{\theta}}_k^i)} = \frac{\prod_m^M p\left(\bar{z}_{m,k} - \bar{z}_{m,k}^i\right)}{\sum_{i=1}^N \prod_m^M p\left(\bar{z}_{m,k} - \bar{z}_{m,k}^i\right)} \quad (12)$$

A number of resampling methods can be used to redistribute the particles and accurately model the multi-variate PDF of the state vector and avoid degeneracy problem [28]. The state estimation is eventually given by the weighted average of the generated particles. Given a sufficient number of generated particles, the covariance matrix $\mathbf{P}_k$ (associated to the state estimate $\hat{\boldsymbol{\theta}}_k$) can be estimated through the *sample covariance* over the set of output particles, $\boldsymbol{\theta}_k^i$. To achieve an optimised PF implementation for DGNSS-CP, the GNSS pseudoranges (and Doppler) measurements and the auxiliary inter-agent distances can be respectively processed as Gaussian-distributed and non-Gaussian-distributed measurements, by exploiting two different likelihood functions $\mathcal{L}(\mathbf{z}_k|\hat{\boldsymbol{\theta}}_k^i)$ and $\mathcal{L}(\mathbf{d}_k|\hat{\boldsymbol{\theta}}_k^i)$, obtained in turn through the related PDFs

$$p(\mathbf{z}_k|\hat{\boldsymbol{\theta}}_k^i) \sim \mathcal{N}(0, \mathbf{R}_{z,k}) \quad (13)$$

$$p(\mathbf{d}_k|\hat{\boldsymbol{\theta}}_k^i) \sim \mathcal{D}(0, \mathbf{R}_{d,k}). \quad (14)$$

The matrices $\mathbf{R}_z$ and $\mathbf{R}_d$ are the *observation noise covariance* matrices and $\mathcal{D}(0, \mathbf{R}_d)$ is a generic non-Gaussian, non-stationary distribution which is expected to be automatically identified (or at least approximated). The two likelihoods are then combined and employed for the weight computation.

III. Methodology

Previous investigations showed that a considerable improvement in estimation accuracy was obtained by choosing proper error PDFs for different parts of the travelled trajectory [16]. This approach is based on a-posteriori knowledge only available in simulation environment, therefore it is not suitable for a real implementation. Furthermore, such a choice is intrinsically tied to the specific scenario to which the simulations are referred. The architecture proposed in this paper aims instead at a real-time likelihood selection based on proximity of the agents only, therefore is a more flexible strategy that can be applied to any kinematic scenario. According to these observations, a set of suitable models has been identified by applying a statistical classification via Monte Carlo simulations. The proposed approach aimed then at describing the dependency between the transition among different error PDFs and a given heuristic to be used to trigger the switch among the available models. It is worth mentioning that GNSS pseudorange and Doppler measurements were considered to be affected by an error modelled as a random variable with Gaussian PDF [2].

A. Mahalanobis distance to model PDF transitions

Early studies showed that the error on the Euclidean Distance between two multivariate random vectors changes its PDF according to the Batthacharyya distance between their statistical distributions [29]. By keeping constant the conditions of the experiment and moving two agents further at each time instant the behaviour of the estimation error follows the trend shown in Figure 3. Due to the fact that the information

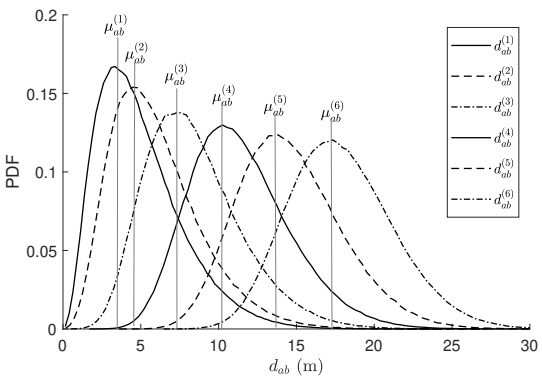

Fig. 3: PDFs of the inter-agent distances computed in a simulated environment. The skewness of the PDF reduces with the increase of the mean μ_i.

related to the positioning solutions of the cooperating agents is unknown at the time of the estimation of their inter-agent distance, we aim at computing a meaningful metric relying on the observables and on the output of the Differential Unit (DU) (implementing the estimation of DGNSS inter-agent distances), $\hat{d}$, and covariance $\mathbf{R}_d$, show in Figure 2. To the purpose, a *statistical distance*, known as *Mahalanobis distance*, is proposed to automatically trigger a mechanism named *Likelihood switch* and detailed hereafter. Such a simple metric is popular in literature for position-related applications such as collision avoidance [30], [31] and motion planning [32]. The generic Mahalanobis distance (a.k.a. Generalized Squared Interpoint Distance) is computed to measure a statistical distance of the observation $\mathbf{x} = [x_1, x_2, x_3, \ldots, x_N]$ from a set of observations with mean $\boldsymbol{\mu} = [\mu_1, \mu_2, \mu_3, \ldots, \mu_N]$ and covariance matrix $\mathbf{R}$, and is defined as $M_d = \sqrt{(x-\mu)^\top \mathbf{R} (x-\mu)}$. It can be considered as a restriction of the Batthacharyya distance which instead provides the statistical distance between two distributions. Indeed, differently from the Euclidean distance, both Batthacharyya and Mahalanobis distances consider the covariance terms of the observations, as depicted in Figure 4. The Mahalanobis distance, M_d, is used in this study to measure the distance of the baseline length distribution from the origin, in the modified form

$$M_d = \sqrt{\left(\mathbf{0}_{1\times k} - \hat{\mathbf{d}}_{ab}\right)^\top \mathbf{R}_d^{(\nabla\Delta)} \left(\mathbf{0}_{1\times k} - \hat{\mathbf{d}}_{ab}\right)} \quad (15)$$

and it provides a statistical magnitude of the distance between two agents. It has to be remarked that

- if the error covariance matrix, $\mathbf{R}_d^{(\nabla\Delta)}$ is the identity matrix, M_d reduces to the *Euclidean distance*.
- if the covariance matrix, $\mathbf{R}_d^{(\nabla\Delta)}$, is diagonal, then the resulting distance is called a *standardised Euclidean distance*

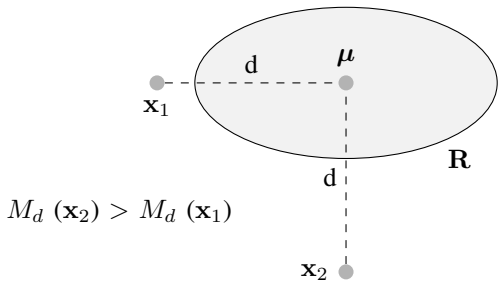

Fig. 4: Comparison of the Mahalanobis distances evaluated between two points $\mathbf{x}_1$, $\mathbf{x}_2$ located at the same Euclidean distance from the mean μ of the distribution.

Figure 5 shows the theoretical behaviour of the M_d obtained through a Monte Carlo simulation over 10^5 samples of a baseline vector perturbed by axial-independent Additive White Gaussian Noise (AWGN) terms, by varying both the magnitude of the baseline vector and ψ_2 of the covariance matrix. It can be observed how the statistical distance from the origin

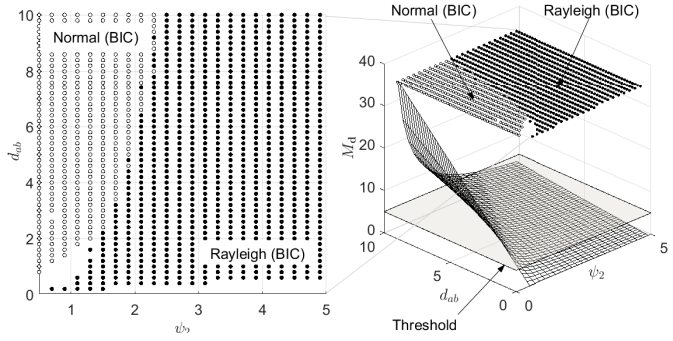

Fig. 5: BIC classification between Normal (empty markers) and Rayleigh (filled markers) PDFs, by varying the magnitude of the inter-agent distance and its error covariance over 10^4 Monte Carlo samples per evaluation point. Mahalanobis distance of (2) from the origin varying baseline length statistics through d_{ab} and ψ_2 (3D plot).

intuitively increases when the actual distance d_{ab} increases, and further increases for small values of ψ_2. According to this metric, the best statistical fit for the error distribution of the baseline length can be analysed as discussed hereafter.

B. Bayesian Inference Criterion for PDF classification

The Bayesian Information Criterion (BIC) can be used to classify the PDF of a given distribution considering a set of possible fitting models [33], [34], and varying M_d. The corresponding likelihood for a given model μ is computed as

$$\beta_\mu = -2\Lambda_\mu + W_\mu \log(L) \tag{16}$$

where Λ_i is the log-likelihood of a given fit model, W is the number of the modelling parameters for the corresponding PDF and L is the number of data points. The BIC uses the optimal value of the log-likelihood function and penalises for more complex models, i.e., models with additional parameters. This approach hence considers *goodness-of-fit* and *parsimony*

BIC-Matching model	Agent 1 (%)	Agent 2 (%)	Agent 3 (%)
GEV	40.47	44.40	36.35
T-loc Scale	-	3.14	2.75
Rayleigh	59.53	30.45	60.90
Normal	-	-	-

TABLE I: Occurrence percentage of pre-defined PDF models for the inter-agent distances computed through W-DDR, for pairwise cooperating agents on a sample trajectory [16].

and it favours models that minimise the complexity. Despite this aspect has been discussed as a potential drawback [35], the proposed BIC classification is hence suitable for the actual implementation in navigation filters.

In Figure 5, it can be observed that for higher values of M_d, the suggested PDF changes according to the value assumed by β. In the trivial case of a diagonal error covariance matrix describing independent terms in (2), a switch between Rayleigh and Gaussian PDFs is observed and is depicted w.r.t. M_d in Figure 5. By considering the previous assumptions made on the error covariance properties, a threshold T_M can be defined based on M_d to operate the actual PDF switch. It can be observed that for $M_D \simeq 3$ where the value of β assumed by the two models is similar, the PDF best fit changes from a Rayleigh to a Gaussian PDF, as shown in Figure 6. A theoretical analysis of the candidate PDF for

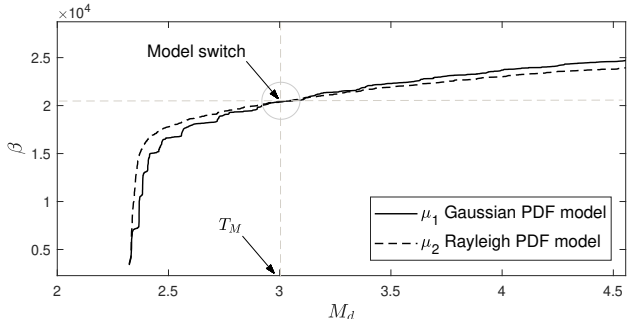

Fig. 6: Approximation of the optimal threshold T_M through the intersection of the BIC likelihood, (16), computed for two PDF models.

the differential inter-agent distances was required through analytical simulations which took into account pre-defined trajectories and properly randomised satellites visibility conditions. Preliminary investigations about the error distribution of DGNSS range measurements provided that W-DDR measurements can be reliably modelled through Generalized Extreme Values (GEV) or Rayleigh distributions when they are obtained from Gaussian-distributed input pseudoranges [12], as supported by the occurrences reported in Table I. The fact that the off-diagonal terms of the error covariance matrix cannot be neglected modifies the best matching distribution from Gaussian to GEV. Both the selected distributions depend on two parameters (ξ for GEV and σ for Rayleigh) which modify the shape of their PDFs. When the two distribution models are integrated in the C-PF, these parameters affect

the generation of the likelihood, the weights computation, and eventually the accuracy and precision of the state estimation.

C. Automated Adaptive Likelihood Switch in C-PF

Two approaches can be addressed for the determination of a matching PDF: (a) a statistical analysis based on multiple samples of the inter-agent distance and a BIC-based discrimination or (b) a threshold-based switch relying on the statistical distance proposed in Section II-B. The approach (b) is hereafter discussed through the Automated Adaptive Likelihood Switch (AALS) algorithm. Referring to the general architecture in Figure 2, an Hybrid PF was equipped with an additional stage devoted to the computation of M_d and a threshold was set according to preliminary simulations in different condition. A previous implementation of a sub-optimal PF architecture revealed remarkable improvement in accuracy when the cooperating agents were far from each other, thanks to the reliability of a Gaussian approximation of the baseline length error and to its negligible non-stationarity [36]. In case of a pass-by instead (e.g. vehicle overtaking a second vehicle), the overall performance was reduced due to the introduction of non-negligible mismodeling of the error PDF in the collaborative measurements. Threfore, the architecture proposed in this paper includes the AALS to limit accuracy drops in the state estimation due to badly modelled PDF functions for the incoming collaborative measurements. According to the fundamental findings of the previous section, the algorithm computes M_d at each epoch and switches among different predefined PDF models. The pseudocode in Algorithm 1 shows the binary likelihood classification performed on top of the computation of M_d, given the estimates of the inter-agent distance and the associated covariance for each of the $M-S$ cooperative measurements.

Algorithm 1 AALS

if $N > 0$ **then**
  for $i = 1 : N$ **do** $M_d = f\left(\hat{\mathbf{d}}_i^{(k)}, \hat{\mathbf{R}}_d^{(k)}\right)$
    if $M_d > T_M$ **then** DistrType $\leftarrow 1$; ▷ GEV
    else DistrType $\leftarrow 2$; ▷ Rayleigh
    end if
    ProbCOOP(:,i)=Likelihood(DistrType,ξ_{GEV},σ_{RAY})
  end for
end if

IV. Results

In realistic scenarios, the error covariance matrix associated to the inter-agent distance is non diagonal and the off-diagonal terms are non-negligible. No assumptions can be made on the error correlation which strictly depends on the geometry of the scenario, as recalled in Section II.

A. AALS in realistic overtaking manoeuvre

A sample scenario is analysed hereafter by considering an overtaking manoeuvre for two cooperating vehicles, as depicted in Figure 7 (top plot). A BIC-based classification of the PDF of the inter-agent distance between A and B was provided as a baseline to identify the switching instants from GEV to Rayleigh PDF (mid plot). The proposed AALS was used to automatically operate the switch between the aforementioned models, by setting the threshold $T_M = 3$. As it can be noticed by comparing mid and bottom plots of Figure 7, the switch was operated over a window that was slightly wider w.r.t. the one identified by the reference BIC classification.

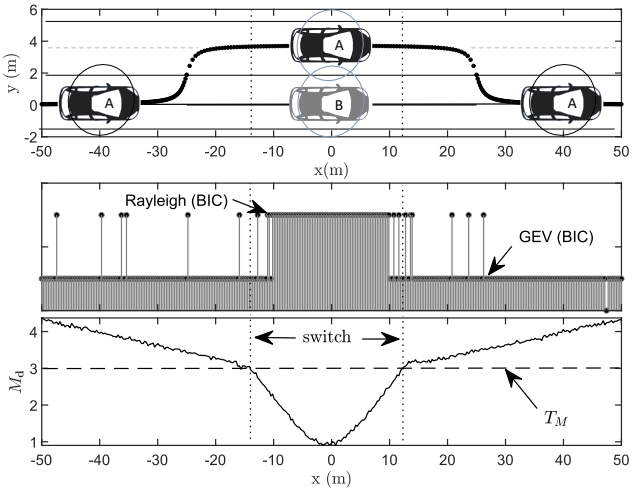

Fig. 7: Comparison of the off-line BIC classification between Rayleigh and GEV PDF (mid plot), and the proposed AALS (bottom plot) analysed for an overtaking scenario (top plot), with realistic error covariances.

Likelihood Selection	50-th PCTL	75-th PCTL	95-th PCTL
Fixed	1.98 m	2.68 m	3.92 m
AALS	1.94 m	2.57 m	3.83 m
Improvement	1.87 %	3.96 %	2.19 %

TABLE II: Percentiles of the Cumulative Density Function (CDF) of the error on the positioning solution computed using different likelihood selection strategies. Percentiles are indicated as PCTL.

B. Position accuracy in realistic kinematic scenarios

The performance of the AALS algorithm were further tested on a realistic scenario, involving a platoon of aiding agents moving counter clock-wise on a circular trajectory and a target agent moving clock-wise on a parallel round trajectory on the opposite lane. The accuracy improvement, which can be seen from Table II, were obtained for a set of $S = 8$ visible satellites simulated through realistic RF signals and by exploiting only one additional inter-agent distance (i.e. a worst-case scenario in terms of network cooperation). The fixed likelihood selection strategy used a GEV distribution with shape parameter $\xi = 0$ for the cooperative measurements for the entire simulation. The AALS instead performed a switch to shape parameter $\xi = 1$ only for those epochs when the computed M_d was below the given threshold, while $\xi = 0$ was identified for all the other cases.

V. Conclusions

This paper describes helpful methodologies to monitor the behaviour of non-stationary cooperative inter-agent distances. It contextually provides an heuristic to classify their error PDF when they are obtained through DGNSS-inherited W-DDR, according to relative geometry of collaborative terrestrial agents and available GNSS satellites. The AALS algorithm, based on the Mahalanobis distance and designed to complement C-PF, is capable to classify the best-matching PDF among a set of pre-defined models, thus improving localisation accuracy in kinematic environment and requiring a limited computational overhead. Despite of the specificity of the results presented in this work, the proposed methodology can generally hold for any inter-agent distance being indirectly computed via Euclidean norm of the baseline vectors (e.g. single difference ranging). In the specific context of DGNSS-CP, the proposed solution guarantees continuity and reliability by avoiding degraded integration of the auxiliary measurements when statistical mismodeling is encountered.

References

[1] X. Cheng, C. Chen, W. Zhang, and Y. Yang, "5G-enabled cooperative intelligent vehicular (5genciv) framework: When Benz meets Marconi," *IEEE Intelligent Systems*, vol. 32, no. 3, pp. 53–59, 2017.

[2] E. D. Kaplan and C. Hegarty, *Understanding GPS/GNSS: principles and applications*. Artech House, 2017.

[3] D. Dardari, E. Falletti, and M. Luise, *Satellite and terrestrial radio positioning techniques: a signal processing perspective*. Academic Press, 2012.

[4] A. Minetto and F. Dovis, "On the information carried by correlated collaborative ranging measurements for hybrid positioning," *IEEE Transactions on Vehicular Technology*, vol. 69, no. 2, pp. 1419–1427, Dec. 2019.

[5] A. I. Mourikis and S. I. Roumeliotis, "Performance analysis of multi-robot cooperative localization," *IEEE Transactions on Robotics*, vol. 22, no. 4, pp. 666–681, Aug. 2006.

[6] K. Liu, H. B. Lim, E. Frazzoli, H. Ji, and V. C. S. Lee, "Improving positioning accuracy using GPS pseudorange measurements for cooperative vehicular localization," *IEEE Transactions on Vehicular Technology*, vol. 63, no. 6, pp. 2544–2556, Jul. 2014.

[7] M. Ilyas, *The handbook of ad hoc wireless networks*. CRC press, 2017.

[8] E. Ahmed and H. Gharavi, "Cooperative vehicular networking: A survey," *IEEE Transactions on Intelligent Transportation Systems*, vol. 19, no. 3, pp. 996–1014, Feb. 2018.

[9] G. M. Hoang, B. Denis, J. Härri, and D. T. M. Slock, "Cooperative localization in GNSS-aided VANETs with accurate IR-UWB range measurements," in *2016 13th Workshop on Positioning, Navigation and Communications (WPNC)*, 2016, pp. 1–6.

[10] F. de Ponte Müller, "Survey on ranging sensors and cooperative techniques for relative positioning of vehicles," *Sensors*, vol. 17, no. 2, p. 271, Jan 2017. [Online]. Available: http://dx.doi.org/10.3390/s17020271

[11] N. Alam, A. Tabatabaei Balaei, and A. G. Dempster, "Relative positioning enhancement in VANETs: A tight integration approach," *IEEE Transactions on Intelligent Transportation Systems*, vol. 14, no. 1, pp. 47–55, Mar. 2013.

[12] A. Minetto, "GNSS-only collaborative positioning methods for networked receivers, doctoral thesis," Ph.D. dissertation, Politecnico di Torino, 2020.

[13] P. Misra and P. Enge, *Global Positioning System: Signals, Measurements and Performance Second Edition*. Lincoln, MA: Ganga-Jamuna Press, 2006.

[14] D. Simon, *Optimal state estimation: Kalman, H infinity, and nonlinear approaches*. John Wiley & Sons, 2006.

[15] A. Doucet and A. M. Johansen, "A tutorial on particle filtering and smoothing: Fifteen years later," *Handbook of nonlinear filtering*, vol. 12, no. 656-704, p. 3, 2009.

[16] A. Minetto, A. Gurrieri, and F. Dovis, "A cognitive particle filter for collaborative dgnss positioning," *IEEE Access*, vol. 8, pp. 194 765–194 779, Oct. 2020.

[17] F. de Ponte Müller, A. Steingass, and T. Strang, "Zero-baseline measurements for relative positioning in vehicular environments," in *Sixth European Workshop on GNSS Signals and Signal Processing*, 2013.

[18] M. Tahir, S. S. Afzal, M. S. Chughtai, and K. Ali, "On the accuracy of inter-vehicular range measurements using GNSS observables in a cooperative framework," *IEEE Transactions on Intelligent Transportation Systems*, pp. 1–10, Jun. 2018.

[19] N. Gogoi, A. Minetto, and F. Dovis, "On the cooperative ranging between android smartphones sharing raw GNSS measurements," in *Proceedings of VTC2019-Fall Honolulu Intelligent Connection and Transportation)*, Sep. 2019.

[20] D. Paindaveine, "A canonical definition of shape," *Statistics & probability letters*, vol. 78, no. 14, pp. 2240–2247, 2008.

[21] L. Dümbgen, "On Tyler's M-functional of scatter in high dimension," *Annals of the Institute of Statistical Mathematics*, vol. 50, no. 3, pp. 471–491, 1998.

[22] D. E. Tyler, "Robustness and efficiency properties of scatter matrices," *Biometrika*, vol. 70, no. 2, pp. 411–420, 1983.

[23] M. Hallin, D. Paindaveine *et al.*, "Optimal rank-based tests for homogeneity of scatter," *The Annals of Statistics*, vol. 36, no. 3, pp. 1261–1298, 2008.

[24] M. Salibián-Barrera, S. Van Aelst, and G. Willems, "Principal components analysis based on multivariate mm estimators with fast and robust bootstrap," *Journal of the American Statistical Association*, vol. 101, no. 475, pp. 1198–1211, 2006.

[25] S. Taskinen, C. Croux, A. Kankainen, E. Ollila, and H. Oja, "Influence functions and efficiencies of the canonical correlation and vector estimates based on scatter and shape matrices," *Journal of Multivariate Analysis*, vol. 97, no. 2, pp. 359–384, 2006.

[26] K. S. Tatsuoka and D. E. Tyler, "On the uniqueness of S-functionals and M-functionals under nonelliptical distributions," *Annals of Statistics*, pp. 1219–1243, 2000.

[27] F. Sottile, H. Wymeersch, M. A. Caceres, and M. A. Spirito, "Hybrid GNSS-terrestrial cooperative positioning based on particle filter," in *2011 IEEE Global Telecommunications Conference - GLOBECOM 2011*, Dec. 2011, pp. 1–5.

[28] T. Li, M. Bolic, and P. M. Djuric, "Resampling methods for particle filtering: classification, implementation, and strategies," *IEEE Signal Processing Magazine*, vol. 32, no. 3, pp. 70–86, 2015.

[29] A. Minetto, C. Cristodaro, and F. Dovis, "A collaborative method for GNSS-based inter-agent range estimation and hybrid positioning algorithm in harsh environment," in *Proceedings of the 30th International Technical Meeting of The Satellite Division of the Institute of Navigation (ION GNSS+ 2017) September 25 - 29, 2017 Oregon Convention Center Portland, Oregon*. Institute of Navigation, 2017, pp. 3784 – 3795.

[30] N. Das and M. Yip, "Learning-based proxy collision detection for robot motion planning applications," *IEEE Transactions on Robotics*, pp. 1–19, Mar. 2020.

[31] S. Alfano and D. Oltrogge, "Probability of collision: Valuation, variability, visualization, and validity," *Acta Astronautica*, vol. 148, pp. 301–316, 2018.

[32] F. Kanehiro, K. Fujiwara, H. Hirukawa, S. Nakaoka, and M. Morisawa, "Getting up motion planning using mahalanobis distance," in *Proceedings 2007 IEEE International Conference on Robotics and Automation*, 2007, pp. 2540–2545.

[33] H. S. Bhat and N. Kumar, "On the derivation of the Bayesian Information Criterion," *School of Natural Sciences, University of California*, vol. 99, 2010.

[34] A. A. Neath and J. E. Cavanaugh, "The Bayesian Information Criterion: background, derivation, and applications," *Wiley Interdisciplinary Reviews: Computational Statistics*, vol. 4, no. 2, pp. 199–203, 2012.

[35] D. L. Weakliem, "A critique of the Bayesian Information Criterion for model selection," *Sociological Methods & Research*, vol. 27, no. 3, pp. 359–397, 1999. [Online]. Available: https://doi.org/10.1177/0049124199027003002

[36] A. Minetto, G. Falco, and F. Dovis, "On the trade-off between computational complexity and collaborative GNSS hybridization," in *2019 IEEE 90th Vehicular Technology Conference (VTC2019-Fall)*, Sep. 2019, pp. 1–5.